Submitted to Journal of Computational Physics

LBL-4814
Preprint

NUMERICAL SOLUTION OF THE HELMHOLTZ EQUATION FOR TWO DIMENSIONAL POLYGONAL REGIONS

Joseph V. Lepore and Robert J. Riddell, Jr.

March 24, 1976

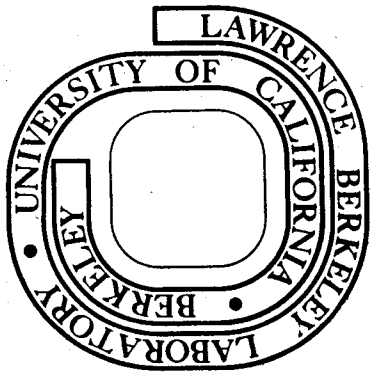

Prepared for the U. S. Energy Research and Development Administration under Contract W-7405-ENG-48

DISCLAIMER

NUMERICAL SOLUTION OF THE HELMHOLTZ EQUATION FOR TWO DIMENSIONAL POLYGONAL REGIONS*

Joseph V. Lepore and Robert J. Riddell, Jr.

Lawrence Berkeley Laboratory
University of California
Berkeley, California 94720

March 24, 1976

ABSTRACT

The Helmholtz equation together with associated boundary conditions can be solved using a dipole distribution on the boundary of any region of interest. If the region has corners, the distribution satisfies a singular integral equation. In this paper numerical techniques for the solution of this equation which take into account the analytic properties of the solution are discussed. Although a complete error analysis has not been developed, some indicators of the errors generated are considered. The technique is illustrated by comparing the numerical solution of the eigenvalue problem associated with various two-dimensional polygonal regions with exact solutions.

I. INTRODUCTION

In a recent article, we have analyzed the solution of the Helmholtz equation for two dimensional regions with corners [1]. In that method the solution was given in terms of a boundary dipole distribution, D, which must be determined in order to satisfy the boundary conditions. It was shown that D satisfies a singular integral equation which can be solved using techniques which have been developed for such equations; these techniques showed that in the vicinity of a corner D has a nonanalytic behavior. The method was illustrated by results which were obtained for the eigenvalues of the Laplacian for various regions, each of which either could also be found analytically or had been studied previously in the published literature. These results, which were obtained using a computer program of general applicability, were very competitive with comparable programs using finite element or finite difference techniques.

In view of this successful application of the boundary distribution technique to the solution of the Helmholtz equation, we feel that it is desirable to describe some of the specific techniques employed in achieving the results. Thus, in this paper we will present some of the methods which were used in solving the singular integral equation for the dipole distribution. In Section II we give the basic results of the previous analysis of this equation, and then in subsequent sections various aspects of the computation are discussed together with a consideration of the accuracy of the solution.

II. BASIC RESULTS FOR THE INTEGRAL EQUATION

The method which we have used for the solution of the boundary-value problem for the Helmholtz equation is based on the classic solutions to the Dirichlet and Neumann problems in which a dipole distribution, automatically satisfying the Helmholtz equation, is introduced on the boundary. The boundary conditions are then expressed in terms of an integral equation for the distribution. For the solution inside a region, one can write:

$$\psi(\vec{r}) = -\frac{\kappa}{4} \oint_C \frac{N_1(\kappa\,|\vec{r}' - \vec{r}|)}{|\vec{r}' - \vec{r}|} D(\vec{r}')(\vec{r}' - \vec{r})\cdot d\vec{\sigma}' , \qquad (1)$$

where $\psi(\vec{r})$ is the solution of the equation

$$(\nabla^2 + \kappa^2)\psi(\vec{r}) = 0 ,$$

$N_1(x)$ is the Neumann function of first order, $D(\vec{r}')$ is the dipole distribution on the boundary at $\vec{r}'$, the integration element $d\vec{\sigma}'$ is a vector in the direction of the outward normal to the boundary and of magnitude equal to the differential path length, ds', on the boundary. The integral is to be carried over the entire boundary, C, enclosing the region. To express the boundary condition, we let $\vec{r}$ approach the boundary. Thus if the boundary is taken as the limit for $\vec{r}$ from the inside of C,

$$\psi_C(\vec{r}) = \frac{D(\vec{r})}{2} - \frac{\kappa}{4} P \oint_C \frac{N_1(\kappa\,|\vec{r}' - \vec{r}|)}{|\vec{r}' - \vec{r}|} D(\vec{r}')(\vec{r}' - \vec{r})\cdot d\vec{\sigma}' , \qquad (2)$$

where $\psi_C(\vec{r})$ is the boundary value for $\psi(\vec{r})$, and the integration is to be carried out for $\vec{r}' \sim \vec{r}$ as a principal value integral. We thus obtain an integral equation for D.

If the boundary is smooth (satisfies a Liapunov condition) it can be shown that the equation is a Fredholm equation and so the usual Fredholm theorems apply to its solution. On the other hand, at a corner the equation is singular and the techniques of singular integral equations [2] must be used. In the previous paper [1] it was shown that in the neighborhood of a corner one could consider an even solution, $D_+(s)$, and an odd solution, $D_-(s)$, on the two sides of the corner, where s is the distance from the corner, and that each would have a series expansion of the form

$$D(s) = \sum d_n s^{\xi_n} , \qquad (3)$$

where the ξ_n are functions of the angle between the sides of the corner, α. Specifically, we found two sequences of ξ_n for each type of solution:

$$\xi_n^{(+)} = \frac{(2n - 1)\pi}{\alpha} , \quad \frac{(2n - 2)\pi}{(2\pi - \alpha)} \qquad (4)$$

and

$$\xi_n^{(-)} = \frac{2n\pi}{\alpha} , \quad \frac{(2n - 1)\pi}{(2\pi - \alpha)} , \qquad (5)$$

where n takes on all nonzero positive integral values. In addition, if two ξ's for the same type of solution are equal, a term of the form $s^{\xi} \log s$ will appear. Further, it was shown that an additional even series of powers of s is generated beginning with each ξ_n.

These results can be compared with what is known for the direct solution of the Helmholtz equation for a bounding wedge of angle α on which the solution vanishes. In this case, expressed in the polar coordinates (r, θ), we have:

$$\psi(r,\theta) = \sum a_n J_{\mu_n}(\kappa r) \sin(\mu_n \theta) ,$$

where

$$\mu_n = \frac{n\pi}{\alpha} , \qquad \frac{n\pi}{2\pi - \alpha} .$$

The first sequence arises if the interior angle, α, is used for the boundary condition on the wedge, while the second arises for the exterior angle, $2\pi - \alpha$. It is seen that the expansion ψ generates the same powers as are found for $D(s)$, except that for $D_+(s)$ a term $\xi_1^{(+)} = 0$ is present and this term would be identically zero in the Bessel expansion for ψ.

III. NUMERICAL TECHNIQUE

We have developed an approximation technique for the solution of Eq. (2) for arbitrary polygons where the sides are straight line segments, and for which $D(s)$ near a corner has the behavior specified by Eq. (3). In reducing the integral equation to an approximate finite form we first introduced a set of points, $\vec{r}_k$, on the boundary for which $D(s_k)$ was to be obtained.

Near a corner we chose N_c points spaced equidistantly on each side of the corner in addition to the corner point itself. Identical treatment on the two sides of a corner greatly facilitated the separation of $D(s)$ into $D_+(s)$ and $D_-(s)$. Some consideration of other than uniform point spacing was made, but no particularly suitable choice seemed indicated. A choice of points analogous to that made in Gaussian integration techniques does not seem to apply here since we are not dealing with an analytic function, and furthermore since $\vec{r}$ appears as a parameter in the integration over $\vec{r}'$,

one might wish to have different points for each $\vec{r}$. The actual corner spacing, h_c, was fixed as

$$h_c = (\ell/(N_d - 2(N_c - 2)) \; (2/N_c)h_f ,$$

where ℓ is the length of the side, N_d is the number of points on the side, and h_f is a free parameter. Thus if $h_f = 1$, h_c is chosen so that the corner points cover a space equivalent to 2 average steps in the remainder of the side, and if $N_c = 2$, h_c will be simply ℓ/N_d. This choice was made to allow simple variation in the number of terms in the corner expansions leaving the mid-range points unaffected.

Once the choice of N_c was made, it was then assumed that the $D_\pm(s)$ could be expanded as:

$$D_+(s) = \sum_{n=1}^{N_c+1} d_n^{(+)} s^{\xi_n^{(+)}}$$

and

$$D_-(s) = \sum_{n=1}^{N_c} d_n^{(-)} s^{\xi_n^{(-)}} ,$$

where the set of ξ's was chosen to be the lowest $N_c + 1$ elements from Eq. (4) or the lowest N_c elements from Eq. (5). It is found that generally the powers of s included do not increase very rapidly and so the various functions, s^ξ, are not very "orthogonal." It is found that, although the lower-powered terms are quite stable in regard to variation of parameters in the calculation, the coefficients of the higher powers tend to vary considerably and show little convergence over the range of parameters used. There is one special case in which convergence was excellent: In order to reduce the

number of points used, the distribution was "mirrored" about one side, thus automatically guaranteeing that $\psi(\vec{r}) = 0$ there. A corner on that side has only $D_-(s)$ different from zero, and if $\alpha = \pi/2$ then $D_-(s)$ has an expansion of only odd integers which was typically highly convergent.

Once the set of points and ξ_n's was chosen, the expansion coefficients were determined by solving the equations:

$$D(s_i) = \sum_{j=1}^{N} d_j (s_i)^{\xi_j}, \qquad i = 1, 2, \cdots, N, \qquad (6)$$

so that the d_j's could be expressed in terms of the $D(s_i)$'s. The lack of orthogonality of the expansion functions could be seen from the relatively large size of some individual elements in the inverse matrix.

For the remaining points on a side, the spacing was chosen to vary linearly from the corner points to the center of the side. This provided some flexibility so that more points could be chosen either near a corner or near the center of a side as desired, or one could chose a uniform spacing if one wished. The parameters were so chosen that the first point away from the N_c corner points would fit as if the corner had two such steps times a free parameter, g_f, while the linear variation in step spacing was chosen so that half the steps on a side would cover half of the side.

The integrals in the integral equation were approximated in two ways, depending on whether the integration variable was near a corner or not. For $\vec{r}'$ not near a corner, the integrand has no

singularity in $D(s')$, while the principal value contribution is zero for a straight side which includes $\vec{r} = \vec{r}'$. Thus we assumed that in this mid-range case the entire integrand could be well approximated by a polynomial of finite degree, and we used a three-point Lagrangian interpolation approximation which was integrated analytically. To minimize truncation error the integration was divided into subpieces each of which had an integration region which was chosen to be symmetric about the central point, thereby eliminating contributions from cubic terms in the integrand. Further, if the step size between points was constant, each sub-integration was carried out from half a step on one side of the center point to half a step on the other side. For nonconstant steps a generalization of this idea was used which still retained the symmetry.

This technique may be contrasted with that used to produce Simpson's rule. In that case, one uses the value of the integrand at three points to construct an approximating quadratic form which is then integrated over the entire region covered by the three points. If one wishes to integrate over a larger region, the next sub-region would include the integrand at the end-point of the sub-region just integrated. In our approximation the approximating quadratic form is constructed as for Simpson's rule, but the integration is only carried out for half a step on either side of the central point, and on moving on to the next sub-region two of the preceding values of the function plus one new evaluation are used to produce the next quadratic approximation. In both techniques the lowest order truncation error is proportional to the quartic term in a Taylor expansion of the function in a sub-region, but one easily finds the magnitude of such

errors is reduced by a factor of 16 in our method as compared with the use of Simpson's rule as described.

For uniform step size, our explicit integration formula is easily found to be:

$$\int_{s_n-h/2}^{s_n+h/2} f(s')ds' \cong \frac{h}{24}\left[f(s_{n-1}) + 22\, f(s_n) + f(s_{n+1})\right] .$$

This approximation, or its generalization for nonuniform steps, was used to integrate over each sub-region with a mid-range point as the center. A 4-point interpolation formula which included cubic terms was also used, and in this case errors similar to those found with the 3-point formula were obtained.

For points $\vec{r}_k'$ near a corner, we assumed that $D(s')$ could be expanded in a finite series of terms of the form $(s')^\xi$, as described above. In additon to the analytic complexity of $D(s)$, the integrand also includes $N_1(x)/x$ in the kernel. This is singular at $x = 0$; since [3]

$$N_1(x) \equiv -2/(\pi x) + (2/\pi)\log x \cdot J_1(x) + \phi(x) ,$$

where $\phi(x)$ is an entire function. The first term in $N_1(x)$ produces the singular behavior of the integral equation at a corner, and this was integrated accurately in conjunction with the expansion for $D(s)$. In the second term, $J_1(x)$ was truncated to two terms of its series expansion, and the remainder of N_1 was assumed to have a power series expansion of a few terms. These, too, were integrated together with the terms s^ξ . These integrals were carried over the

region from the corner to the beginning of the mid-range integration described above.

Specifically, we handled the corner integrals as follows:

A typical integral over the first term in N_1 is of the form

$$I(\vec{r},a,\xi) = \int_0^a \frac{r \sin\theta \cdot s^\xi\, ds}{r^2 - 2rs\cos\theta + s^2} ,$$

where (r,θ) are the polar coordinates of the point $\vec{r}$. This can easily be converted to

$$I(\vec{r},a,\xi) = \mathrm{Im}\left\{ \int_0^a \frac{s^\xi\, ds}{s - r\, e^{i\theta}} \right\} ,$$

and, if $r > a$,

$$I(\vec{r},a,\xi) = -a^\xi\, \mathrm{Im}\left\{ \sum_{n=0}^{\infty} \frac{(a/r\, e^{i\theta})^{n+1}}{n + \xi + 1} \right\} . \qquad (7)$$

For $r > a$, this series can be used to evaluate the integral, although for $r \sim a$ the rate of convergence is slow and an alternative form shown in the appendix was then used. For $r < a$ the series is divergent but we can obtain its analytic continuation by first observing that [4]:

$$\int_0^a \frac{s^\xi\, ds}{s + z} = \frac{a^{\xi+1}}{(\xi+1)z}\, {}_2F_1\left(1,\ \xi+1;\ \xi+2;\ -\frac{a}{z}\right) ,$$

where ${}_2F_1$ is the ordinary hypergeometric function. This expression can be converted into a form useful for computation by using the Kummer relation [5]:

$$ {}_2F_1(1,\ \xi+1;\ \xi+2;\ -\frac{a}{z}) \;=\; \frac{(\xi+1)}{\xi}\left(\frac{z}{a}\right) {}_2F_1(1,\ -\xi;\ 1-\xi;\ -\frac{z}{a}) $$

$$ -\frac{\pi(\xi+1)}{\sin \pi\xi}\left(\frac{z}{a}\right)^{\xi+1} . $$

The new hypergeometric function can then be expanded in a power series in (z/a).

The second term in the expression for $N_1(x)/x$ includes $\log(s^2 - 2sr\cos\theta + r^2)$, and this term can be reduced to the previous forms via an integration by parts. Thus, for example,

$$ \int_0^a s^{\xi} \log(s^2 - 2rs\cos\theta + r^2)\,ds $$

$$ = \frac{a^{\xi+1}}{\xi+1}\log(a^2 - 2ar\cos\theta + r^2) $$

$$ - \frac{2}{\xi+1}\int_0^a \frac{s^{\xi+1}(s - r\cos\theta)}{s^2 - 2rs\cos\theta + r^2}\,ds . $$

The remaining term in $N_1(x)/x$, which is an even polynomial in x, can be integrated directly.

By using these techniques the integral equation was reduced to an approximate set of linear, algebraic equations which could then be solved for $D(s_k)$ using standard methods. This approach has been used to find the eigenvalues of the Laplacian for a variety of polygonal regions. The eigenvalues were determined by finding approximate zeros of the determinant of these equations. Unfortunately,

the kernel in the integral equation involves the eigenvalue, κ, in a complicated way, and so an iteration approach for finding κ was necessary.

IV. RESIDUAL ERRORS

If the technique presented here is to be useful for the solution of practical problems, it seems very desirable to have an estimate of the accuracy achieved for various choices of the parameters in a particular calculation. The method has been applied to find a few eigenvalues for problems with known analytic solutions and this is of course helpful. On the other hand, the eigenvalue as calculated here does not seem to satisfy an extremum condition, and we have seen numerically that by varying the parameter h_f, for example, κ can change from below the correct value to above it. Thus it is very desirable to have some other criterion of accuracy for a solution; presumably one which is more closely related to the solution, $\psi(\vec{r})$.

Unfortunately, the system is quite complicated and we have not succeeded in developing a satisfactory overall error analysis. On the other hand, we have used the methods above described to calculate the value of $\psi(\vec{r})$ at points on the boundary halfway between the points at which $D(s)$ was fixed in the equation. If the solution obtained were exact, these values would all be zero, so the deviation from zero (with the solution normalized to 1 at some central point in the region) presumably indicates the errors present. There is one difficulty with this calculation: Although the integral term in the equation can be calculated in exactly the same fashion regardless of

where the point $\vec{r}$ is located, the term $D(s)/2$ cannot. This term is obtained in the solution at precisely the original points used, but it must be deduced by interpolation or otherwise at the halfway residual points. Thus there is a potential for an additional error generation in the residual ψ calculation which is not present in the original approximating equation. At any rate, the same ideas for the evaluation of $D(s)$ were used for this purpose as went into the original approximating scheme so the result should be meaningful. In particular, for points near a corner we used expansions for $D(s)$ as given by Eq. (6), but in the mid-range, $D(s)$ was interpolated using a 6-point formula after a 4-point formula was found to produce a substantially larger residual ψ.

V. RESULTS

A program has been developed which incorporates the above ideas and it has been applied to a variety of problems, most of which have known analytic eigenfunctions. Results obtained for the eigenvalues for various cases were discussed in [1]. For completeness, some of these results are repeated here in Table I. As has been mentioned already, in order to reduce the number of points in the calculation, we have chosen to generate $\psi(\vec{r})$ by $D(s)$ together with its mirror image as reflected in one side of the figure considered. It is found that results for incompletely symmetric figures, such as the 30°-60°-90° triangle thereby become dependent on which side is used for the reflecting. Thus, in Table I, an indication is stated as to which side was used for the reflection. In this Table, the results were obtained using 5 points near each corner to determine

the expansion in powers of s^ξ, and the parameters h_f and g_f were chosen to be 1.0 and 0.7, respectively. A total of 53 points were used on the boundary to express $D(s)$. For each figure, the longest side was chosen to have unit length.

The analytic value for the lowest eigenvalue for each figure is as follows: Equilateral triangle, $\kappa = 4\pi/\sqrt{3}$; 45° isosceles triangle, $\kappa = \pi\sqrt{5}$; 30°-60°-90° triangle, $\kappa = 4\pi\sqrt{7}/3$; and square, $\kappa = \pi\sqrt{2}$.

In Table II, we show similar results for an equilateral triangle. In this case, we have made calculations for a variety of parameters, N_c, N_d, g_f, and h_f. In this table we also include one higher eigenvalue. This is in good agreement with that found in Table I for the 30°-60°-90° triangle. We also give an eigenvalue which leads to a null solution for $\psi(\vec{r})$, as is more fully discussed in [1].

In this table the significance of the number of points per side, N_d, is clear, and it is seen that the accuracy of the eigenvalue, κ, is greatly enhanced by increasing N_d. The dependence of κ on N_c is not particularly marked, but it will be seen that the residual $\psi(\vec{r})$ is substantially improved as N_c is changed, for example, from $N_c = 3$ to $N_c = 5$. Because of the way in which the parameters enter in the determination of points, the mid-range points are essentially unaffected if $N_d - 2N_c$ is kept fixed. This explains the particular choice made for N_d in the table. The parameter h_f affects primarily the step size in the corner region; as it is decreased the steps are decreased proportionately. Since the mid-range points are linked to the corner points, they are similarly

affected. On the other hand, if g_f is varied the corner points are unaffected while the mid-range points are modified. Evidently if h_f or g_f is reduced the steps near the corners are reduced and so the steps in the middle of a side will be increased. For the choice of these two parameters we have typically found that values larger than 1.0 produced less satisfactory results than did smaller values, with the choice $h_f = 1.0$, $g_f = 0.7$ usually producing a slightly better κ and residual ψ than did $h_f = 0.7$, $g_f = 1.0$.

In Table III we present some calculated values for the expansion coefficients for $D_+(s)$ at the corner not on the "mirror" side. (From symmetry $D_-(s)$ at this corner is zero.) It should be noted that, because of the linearity of the equation for $D(s)$, these coefficients are somewhat arbitrary. They have been fixed by fitting $D(s)$ to a quadratic form near its maximum value; this maximum was then set equal to 1.0. It is seen that for fixed N_c, as the step size in the corner is reduced, the lowest coefficient (which gives $D(s)$ at the corner) is accurately obtained. The second coefficient is quite small and is perhaps converging to zero, while the third coefficient shows good convergence to a finite value. The highest terms are fairly large and since they are of opposite sign they may be indicative of the effect of truncation of the series. In this table we have also given the coefficients for cases in which the number of terms in the expansion is changed, and here, too, it is seen that the lowest coefficient is accurately fixed.

Finally, in the figures we present some results for the residual $\psi(\vec{r})$ as obtained using various choices for the parameters. In each case we have superimposed on the figure the solution for $D(s)$

as a smooth curve. The ψ's are normalized by calculating the value of $\psi(\vec{r})$ at the center of the triangle and then scaling all of the ψ's so that the central value is 1.

In Fig. 1, we present the results for cases in which $N_d = 26, 36, 46$ while $N_c = 5$, $h_f = 0.7$, and $g_f = 1.0$ to illustrate the decline of the residual ψ as the number of points is increased. In Fig. 2 similar results are given for cases in which the number of points in the corner expansion was varied, and, as would be expected, it is seen that the residuals are decreased as N_c is increased. Since these values are essentially the same in the mid-range, we only plot the corner region. It is seen that the largest error in the residual is typically found for the point nearest the corner. This is a common property of the process used here in which the approximating series to a given function is forced to agree at a set of points. Experimentally it was found that functions such as s^η showed the largest error for small s when fitted by the series of Eq. (3), if η was not in the set of ξ_n's used. In Fig. 3 we compare the four cases in which g_f and h_f are each either 0.7 or 1.0. This demonstrated how compression of the point spacings at the corner improves the accuracy there but decreases it in the center of a side.

As was discussed in [1], the integral equation generates both nontrivial eigensolutions of the Helmholtz equation, $\psi_\kappa(\vec{r})$, and also null solutions for $\psi_\lambda(\vec{r})$ for which, however, $D_\lambda(s)$ is not zero. It is found that eigenvalues for these two cases (κ and λ respectively) can be quite close together (see Table I), and that the solutions for $D(s)$ are then very similar. We suggest that the errors

in ψ may be reduced by calculating $\psi_K(\vec{r}) - \psi_\lambda(\vec{r})$, so in Fig. 4 we give both the residual ψ_K and also the difference of ψ_K and ψ_λ for which ψ_λ is normalized using $D_\lambda(s)$, rather than ψ_λ at the center of the triangle, since the latter is $\ll 1.0$. Finally, in Fig. 5 we give the residual ψ calculated for the L-shaped region.

VI. CONCLUSION

In this article we have described techniques which have been developed for the solution of a singular integral equation. This equation arises when a boundary dipole distribution is used to effect the solution of the Helmholtz equation for two-dimensional regions with sharp corners. These techniques make extensive use of analytic properties of the solution of the equation which were deduced in an earlier paper. In particular, these properties include the series of fractional powers in terms of which the solution can be expanded in the vicinity of a corner, and the regular behavior elsewhere on the sides.

Using these techniques we have obtained very accurate results for the eigenvalues of the Laplace operator for various two dimensional polygonal domains. In addition, we have a good indication from the residual ψ values calculated at extra points on the sides that the solution for ψ is quite accurate. We have also shown that the series expansion for $D(s)$ is adequately convergent near a corner, with leading coefficients which are quite stable. Thus we feel that analytic properties can be very successfully invoked in obtaining satisfactory solutions for such equations.

VII. ACKNOWLEDGMENT

The authors would like to express their appreciation for the many helpful conversations which we have had with Dr. Loren Meissner regarding various points in these calculations.

APPENDIX

In the numerical calculations the series of Eq. (7) was used directly for small (a/r). For larger ratios, the convergence of the series becomes very slow, so a modification was made to improve the convergence. Using the identity:

$$\frac{1}{n+\xi} = \frac{1}{n+a} + \frac{(a-\xi)}{(n+\xi)(n+a)},$$

we can obtain

$$\sum_{n=0}^{\infty} \frac{z^n}{n+\xi} = \sum_{n=0}^{\infty} \frac{z^n}{n+1} + (1-\xi)\sum_{n=0}^{\infty} \frac{z^n}{(n+1)(n+2)} + \cdots$$

$$+ (1-\xi)\cdots(k-\xi)\sum_{n=0}^{\infty} \frac{z^n}{(n+1)\cdots(n+k+1)}$$

$$+ (1-\xi)\cdots(k+1-\xi)\sum_{n=0}^{\infty} \frac{z^n}{(n+1)\cdots(n+k+1)(n+\xi)}.$$

Each of the series except the last can be obtained in analytic form, while the final series converges rapidly because of the high power of n which appears in the denominator.

FOOTNOTES AND REFERENCES

* This work supported by the U.S. Energy Research and Development Administration (ERDA) under Contract W-7405-ENG-48.

1. J. V. Lepore and R. J. Riddell, Jr., Boundary Distribution Solution of the Helmholtz Equation for a Region with Corners, Lawrence Berkeley Laboratory Report LBL-4693 (to be published).

2. W. Pogorzelski, Integral Equations and their Applications (Pergamon, Long Island City, N. Y., 1966), p. 230, ff.

3. M. Abramowitz and I. A. Stegun, Handbook of Mathematical Functions (U. S. Government Printing Office, Washington, D. C., 1964), p. 358, Eq. (9.1.11).

4. A. Erdélyi, ed., Higher Transcendental Functions, Vol. I, (McGraw-Hill Book Co., Inc., New York, N. Y., 1953), Sec. 2.12, Eq. (11).

5. This result is easily obtained using Eqs. (9), (13), (34) of Sec. 2.9 and Eq. (6) of Sec. 1.2 of Ref. 4.

TABLE I

Calculated Eigenvalues for Various Figures.

Case	Refl. Side	κ	Error
Equilateral Triangle	Any	7.255218367	2.09×10^{-5}
45°-45°-90°	Long Side	9.934553730	-3.45×10^{-5}
	Short Side	9.933726725	-8.62×10^{-4}
30°-60°-90°	Long Side	11.08250607	8.89×10^{-6}
	Middle Side	11.08234361	-1.54×10^{-4}
	Short Side	11.08187716	-6.20×10^{-4}
Square	Any	4.442863650	-1.93×10^{-5}

TABLE II

Eigenvalues for an Equilateral Triangle.

In all cases $g_f = 0.7$, $h_f = 1.0$.

N_d	N_c	κ	Error
22	3	7.255065020	-1.32×10^{-4}
24	4	7.255144251	-5.32×10^{-5}
26	5	7.255192959	-4.50×10^{-6}
28	6	7.255225547	2.81×10^{-5}
36	5	7.255191813	-5.65×10^{-6}
46	5	7.255194590	-2.87×10^{-6}
		* * * * * * *	
26	5	7.084753232	("Null" case)
26	5	11.08269983	2.03×10^{-4}

TABLE III

Corner Expansion Coefficients.

N_d	N_c	g_f	h_f	d_0	d_1	$d_{1.2}$	d_2	$d_{2.4}$	d_3
22	3	0.7	1.0	-0.1494165	0.016	1.927	4.76		
24	4	0.7	1.0	-0.1494316	0.169	1.528	7.07	- 3.3	
26	5	0.7	1.0	-0.1494506	-0.063	2.225	-1.31	18.2	-22.6
28	6*	0.7	1.0	-0.1494586	-0.026	2.112	0.26	13.1	-18.8
26	5	1.0	0.7	-0.1494551	-0.015	2.075	0.78	12.4	-15.5
36	5	0.7	1.0	-0.1494522	-0.024	2.107	0.14	14.5	-18.7
46	5	0.7	1.0	-0.1494705	-0.013	2.072	0.64	13.1	-17.3
26	5	1.4	0.7	-0.1495963	0.012	1.983	2.51	6.8	- 7.3

* For $N_c = 6$ there is also a coefficient (= -1.74) of a term of the form $s^3 \log s$.

FIGURE CAPTIONS

Fig. 1. Residual $\psi(\vec{r})$ and $D(s)$ on the boundary for an equilateral triangle: $N_d = 26(+)$, $36(\times)$, $46(\diagup)$.

Fig. 2. Residual $\psi(\vec{r})$ and $D(s)$ for an equilateral triangle near a corner. In each case, $g_f = 0.7$, $h_f = 1.0$.

Fig. 3. Residual $\psi(\vec{r})$ and $D(s)$ for an equilateral triangle for various choices of g_f and h_f. In each case, $N_c = 5$, $N_d = 26$.

Fig. 4. Residual $\psi_\kappa(\vec{r})$ and $[\psi_\kappa(\vec{r}) - \psi_\lambda(\vec{r})]$ for $N_c = 5$, $N_d = 26$, $g_f = 0.7$, $h_f = 1.0$ for an equilateral triangle. The solid curve gives $D_\kappa(s)$, and the dashed curve, $D_\lambda(s)$.

Fig. 5. Residual $\psi(r)$ and $D(s)$ for the "L"--shaped region for $N_c = 5$, $N_d = 28$, $g_f = 0.7$, $h_f = 1.0$.

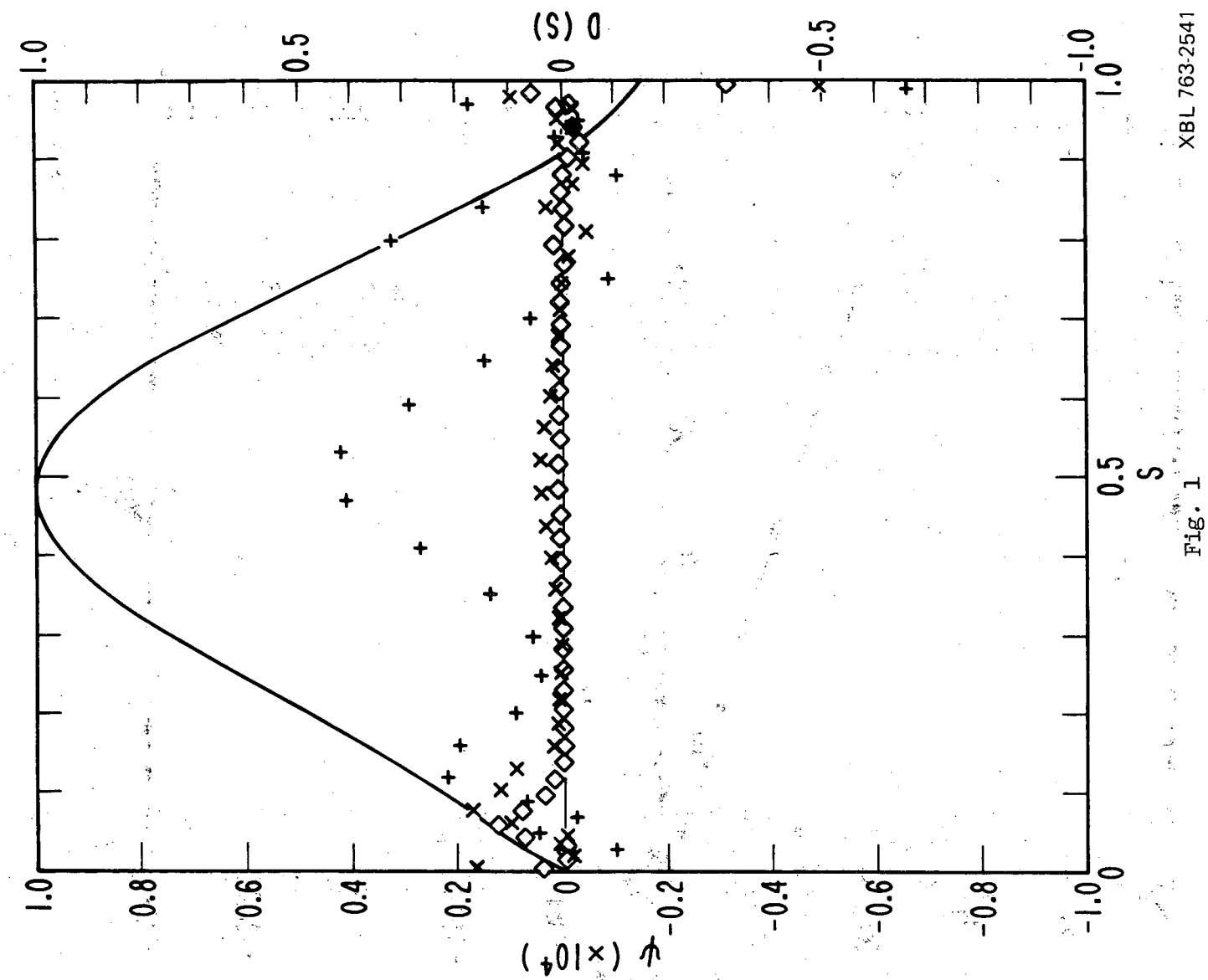

XBL 763-2541

Fig. 1

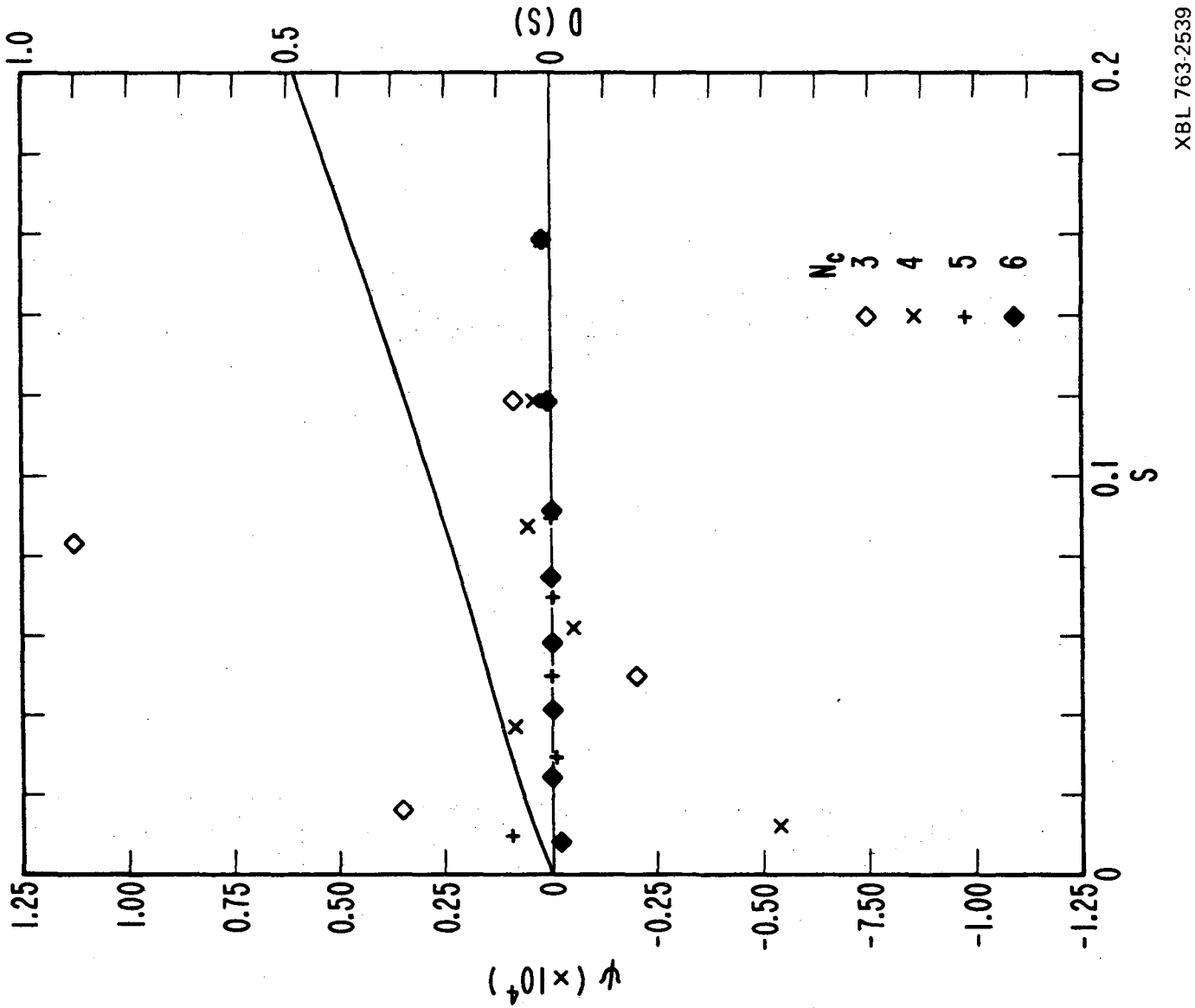

XBL 763-2539

Fig. 2

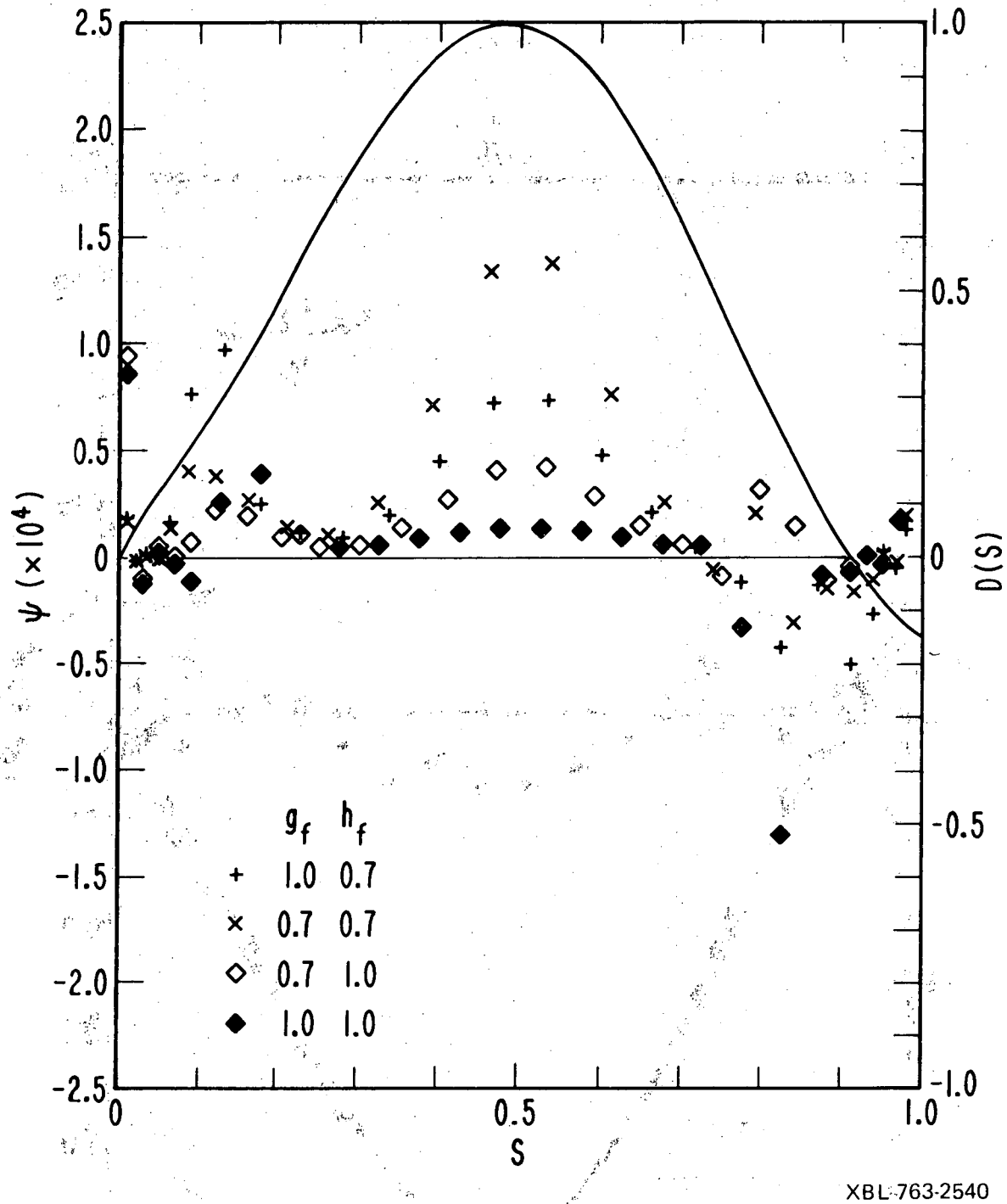

XBL-763-2540

Fig. 3

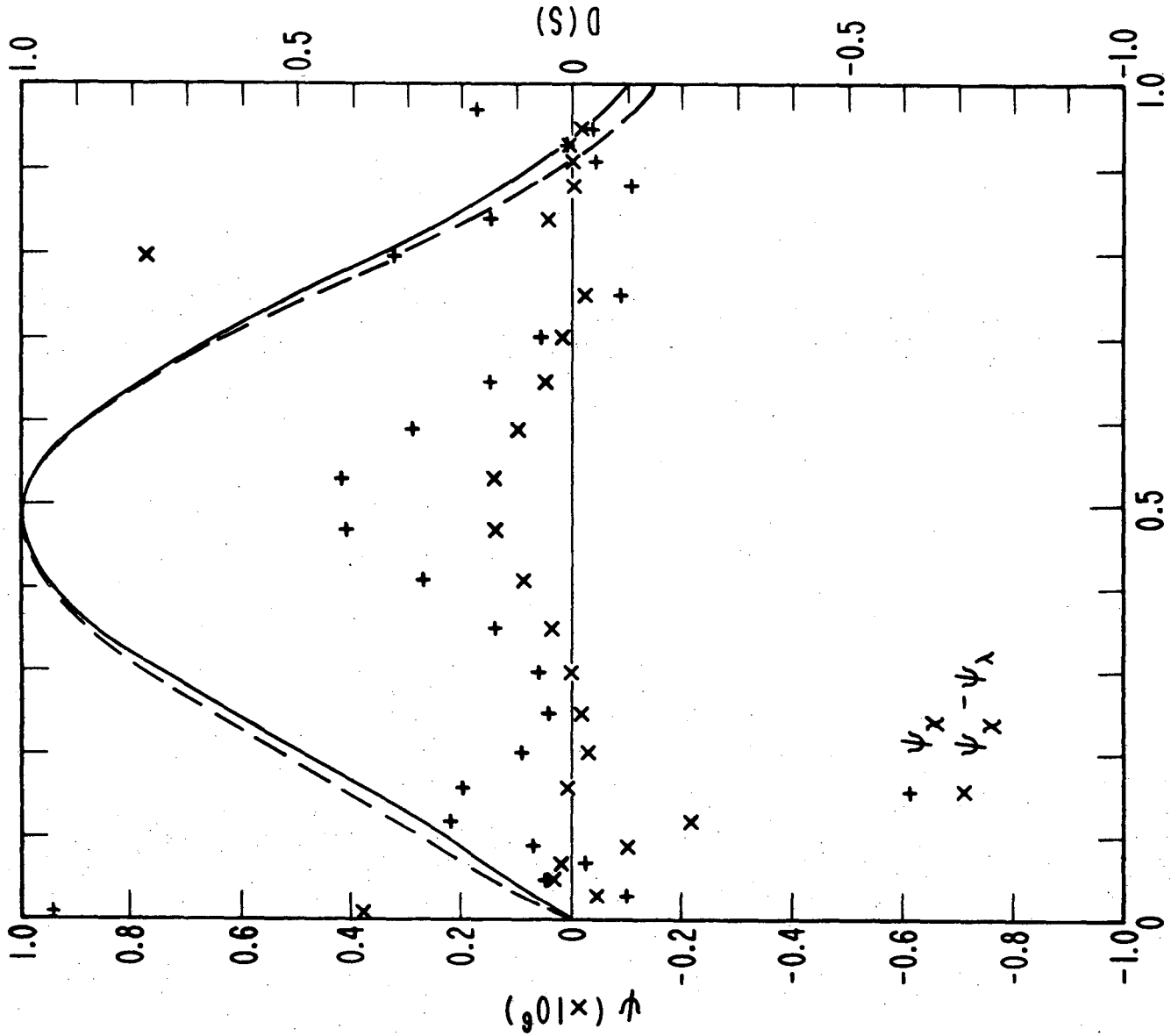

XBL 763-2542

Fig. 4

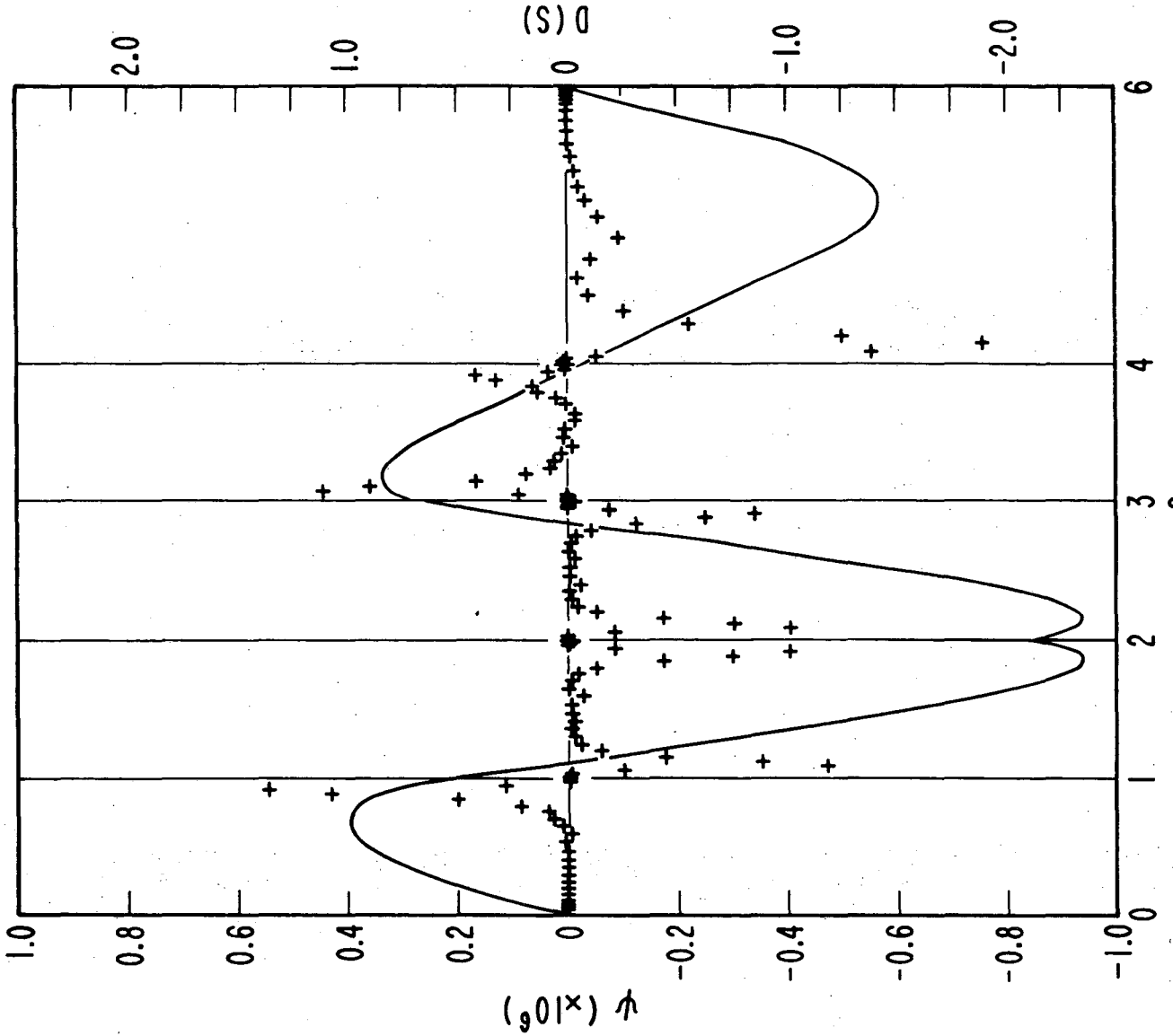

XBL 763-2543

Fig. 5

TECHNICAL INFORMATION DIVISION
LAWRENCE BERKELEY LABORATORY
UNIVERSITY OF CALIFORNIA
BERKELEY, CALIFORNIA 94720